Received: 05 October 2022 | Revised: 19 November 2022 | Accepted: 25 November 2022
DOI: 10.22034/ecc.2023.368472.1545
Eurasian Chemical Communications
SAMI

FULL PAPER

Anticorrosion activity of some new heterocyclic link with imidazo[2,1-b]benzthiazole

Zeena Ali Abdulameer* | **Naeemah Jabbar Al-Lami**

Department of Chemistry, College of Science, University of Baghdad, Baghdad, Iraq

A new series of imidazoles [2,1-b]benzthiazole linked with other heterocyclic scaffolds were synthesized, and a new Mannich base link with a drug (Cefixime) was also synthesized. Oxopyrimidine ring was prepared from reacting Mannich base containing terminal Methyl group condensed with different substituted aromatic aldehydes, producing new chalcones, which undergo ring closer with urea gave new Oxopyrimidine derivatives. All compounds were recognized by Fourier Transform Infrared Spectroscopy, Proton nuclear magnetic resonance and Carbon-13 (C13) nuclear magnetic resonance spectra. Some new compounds were evaluated as anticorrosion agents, and some showed potent inhibition against corrosion.

***Corresponding Author:**
Zeena Ali Abdulameer
Email:zena.ali1205m@sc.uobaghdad.edu.iq
Tel.: +9647722300207

KEYWORDS

Oxopyrimidines; imidazobenzthiazole; anticorrosion.

Introduction

Imidazo-fused heterocyclic scaffolding is one of the most significant core structures in organic molecules, which is present in a wide variety of natural goods and physiologically active substances having antibacterial [1], anticancer [2], antimicrobial [3], antifungal [4], antiviral [5], and anti-inflammatory [6] activities. These are structural motifs of various marketed drugs [7], including divaplon and fasiplon [8]. Imidazo-fused benzothiazoles are quite significant in the pharmaceutical sector [9] for their wide various fascinating pharmacological activities because the reaction might involve various structures, moderate reaction circumstances, and the possibility of further change of the products formed by Mannich bases [10]. One of the most important methods used in contemporary organic chemistry is the Mannich reaction. A variety of biological and pharmacological effects are displayed by Mannich bases, including anti-inflammatory [11], antibacterial [12], antitumor [13], anti-oxidant [14], and antifungal [15]. Mannich bases also act as important pharmacophores or bioactive leads, which are further used for the synthesis of various potential agents of high medicinal value which possess aminoalkyl chains. Examples of clinically useful Mannich bases that consist of an aminoalkyl chain are cocaine, fluoxetine, atropine, ethacrynic acid, trihexyphenidyl, procyclidine, ranitidine, biperiden, and so forth.

There have been several specialized scientific investigations on chalcone chemistry; particularly notable are their uses in biology, industry, and medicine [16]. Because of the chromophore and auxochrome groups [17] in their structures, chalcones are

coloured compounds. They are recognized as derivatives of benzal acetophenone. Chalcone contains a very good synthon, so various new heterocycles with a good pharmaceutical profile can be designed. Chalcones are α-β unsaturated ketones containing the reactive ketoethylenic group –CO-CH=CH-. These are colored compounds because of the presence of the chromophore -CO-CH=CH- which depends on the presence of the other auxochromes.

One of the most active classes of chemicals, Oxopyrimidine and its derivatives exhibit a wide range of biological actions. Derivatives of pyrimidine found in natural materials like nucleic acid have a wide range of biological functions, vitamin B, and they are of exceptional pharmacological value. Several nucleic acid analogues, such as fluorouracil, have been utilized to treat cancer. Because they serve as some of the components of D.N.A. and R.N.A. [18], pyrimidines are one of the chemicals that make life possible.

Aims of work

1) Synthesis of new 5-substituted compounds of 2-aryl imidazo [2,1-b] benzothiazole derivatives.
2) The new aromatic fused ring system will be characterized by C.H.N. analysis and FT-IR, 1H-NMR and 13C-NMR spectra.
3) Evaluation of their applications, such as anticorrosion, antibacterial, and antifungal activities.

Materials and methods

All of the ingredients and solvents were purchased through C.D.H. and Reagent World companies, respectively, and came from Merck Chemicals, B.D.H., and Sigma/Aldrich. Aluminium sheets via the Merck Company that had been pre-coated with silica gel 60 were used for thin-layer chromatography (T.L.C.), and spots were identified using iodine vapours.

Instrumentation

1) The Gallenkamp capillary melting point apparatus was used to measure melting points in an uncorrected manner.
2) To record infrared spectra, the University of Baghdad College of Science used a Shimadzu Fourier Transform Infrared (FT-IR-8400S) Spectrophotometer.
3) Proton nuclear magnetic resonance and Carbon-13 (C13) nuclear magnetic resonance spectra were recorded using the Varian model ultra-shield nuclear magnetic resonance spectrometer, respectively, at 400 and 499.67 MHz and 125 MHz, the use of deuterated dimethyl sulfoxide solvent (DMSO-*d6*).

In Mashhad University, Iran, chemical changes related to the internal reference tetra-methyl silane (T.M.S.) were measured in parts per million (ppm).

Synthesis 6-(4-bromophenyl) imidazo [2, 1-b] benzathiazole (1A) [19]

A mixture of 2-aminobenzothiazole (3 mmol) (0.5 g) and 4-Bromo phenacyl bromide (3 mmol) (0.9 g) was dissolved in EtOH absolute (80-100 mL) before heating under reflux for 13-15 hours. The reaction was monitored by T.L.C. using (EtOAc: petroleum ether; 2:1). The mixture was then filtered and basified with (5% NaOH) until pH reached (10-11). The precipitate was separated, rinsed with hot distilled water, dried, and recrystallized using absolute Ethanol to give yellowish-orange crystals with an 80% yield. Table 1 presents the physical characteristics of this compound (1A).

Synthesis of mannich bases derivatives compounds (2-3) [20]

A mixture of compound 1 (2 mmol) (0.5 g) in EtOH (25 mL) was added to (37%) formaldehyde (2 mmol) and some drops of conc. HCl was added until the pH of the reaction medium became around (4-5), and then the mixture was stirred for 30 minutes.

After that, one of the different primary aromatic amines (2 mmol) (0.2 g) was added and heated for 2-3 hours. After the reflux stopped, allowing the reaction mixture to cool to room temperature, the solid mass was filtered, washed, dried, and purified with EtOH. Table1 provides a list of these compounds' physicochemical characteristics.

Synthesis of chalcones compounds (4-10A)

To a solution of compound (2A) (1 mmol) (0.8 g) in ethanol (15 mL), a solution of 40% NaOH (1mL) was added and stirred for 25-30 min. After that, substituted benzaldehydes (1 mmol) (0.3 g) were added. The resulted mixture was stirred for 24 hours. The products were cooled, filtered, dried, and then recrystallized from ethanol. The physical characteristics of these compounds are listed in Table 1.

Synthesis of Oxopyrimidine compounds (11-17A)

A mixture of chalcones (4A) (3 mmol) (0.3 g) with urea (3 mmol) (0.03 g) and K_2CO_3 (3 mmol) (0.05 g) in ethanol (10 mL) was refluxed for 25 hours. After cooling, the reaction mixture was neutralized with 20% HCl. Filtering and recrystallization of the isolated solid using ethanol-produced compound (5A). Table 1 displays the chemical compound's physical characteristics.

TABLE 1 Physical characteristics of Compounds (1-17A)

Compound No.	Structure	Molecular formula	Molecular Weight (g /mole)	Colour	m.p. (°C)	Time (h)	Yield (%)
1A	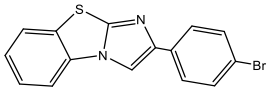	$C_{15}H_9BrN_2S$	329.22	Yellowish -orange	125	13-15	80%
2A	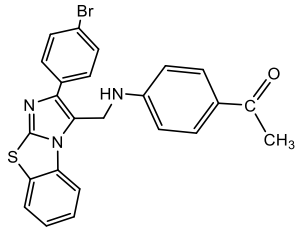	$C_{24}H_{18}BrN_3OS$	476.39	Pale yellow	208	2-3	58%
3A	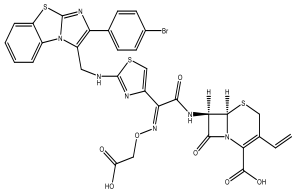	$C_{32}H_{24}BrN_7O_7S_3$	794.67	Off white	160	10	51%
4A	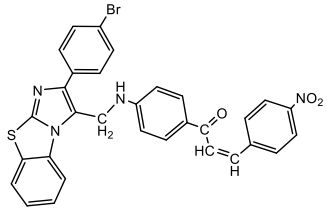	$C_{31}H_{21}BrN_4O_3S$	609.5	Orange	115	24	60%

5A	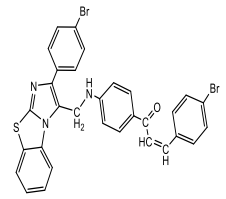	$C_{31}H_{21}Br_2N_3OS$	643.4	Pale yellow	118	24	55%
6A	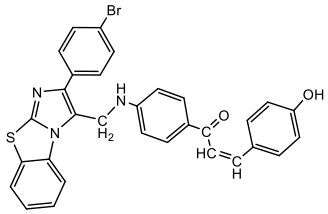	$C_{31}H_{22}BrN_3O_2S$	580.5	Pale yellow	138	24	50%
7A	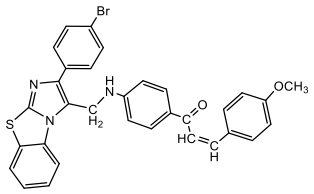	$C_{32}H_{24}BrN_3O_2S$	594.53	Light orange	150	24	52%
8A	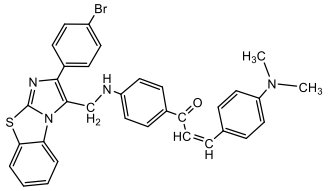	$C_{33}H_{27}BrN_4OS$	607.57	Orange	156	24	55%
9A	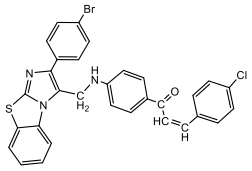	$C_{31}H_{21}BrClN_3OS$	598.94	Yellow	176	24	75%
10A	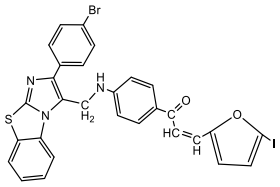	$C_{29}H_{23}BrIN_3O_2S$	684.39	Black	277	24	88%
11A	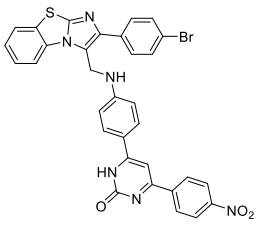	$C_{32}H_{21}BrN_6O_3S$	649.52	Light orange	145	25	77%
12A	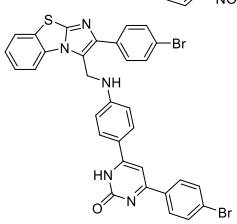	$C_{32}H_{21}Br_2N_5OS$	683.42	Pale yellow	230	22	75%

13A	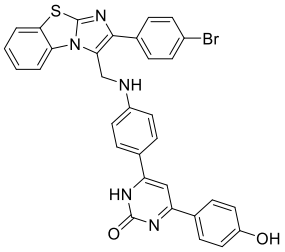	$C_{32}H_{22}BrN_5O_2S$	620.53	Brown	300	22	96%
14A	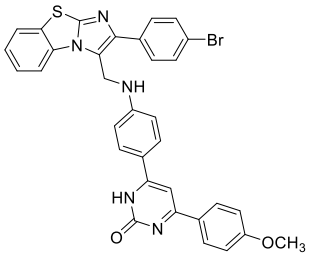	$C_{33}H_{24}BrN_5O_2S$	634.55	Orange	200	22	70%
15A	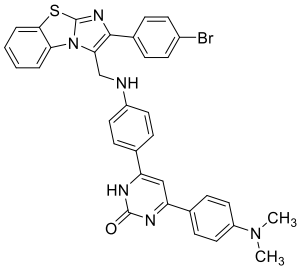	$C_{34}H_{27}BrN_6OS$	647.60	Pale Orange	195	22	89%
16A	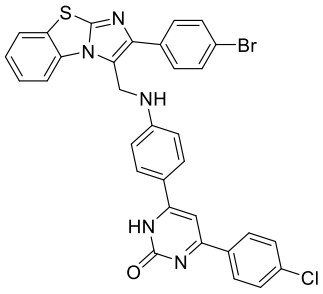	$C_{32}H_{21}BrClN_5OS$	638.97	Light Yellow	280	22	95%
17A	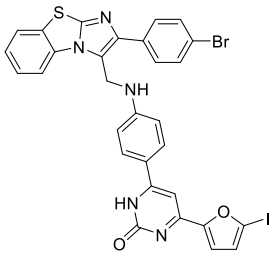	$C_{30}H_{23}BrIN_5O_2S$	724.24	Light Brown	219	25	95%

Results and discussion

Compound (1A) production is a documented process in the literature [21] and is accepted by Fourier Transform Infrared Spectroscopy spectrum data, which includes the disappearance of the (NH_2) band at (3400) cm^{-1} and the (C=O) band at (1700) cm^{-1} and the debut of brand-new bands of (C=N) imidazo at (1679-1662) cm^{-1} related to the imidazole ring's development; as shown in Table 2.

The reaction of novel Mannich bases was the second step, which involved compound (1A) with formaldehyde (37%) and different primary aromatic amines to produce compounds (2-3A), The FT-IR of Mannich

bases derivatives showed new stretching bands (N-H) 3290-3396 cm^{-1}, and also (C-H) aromatic bands at (3066-3095) cm^{-1}, and (C-H) aliphatic bands at (2968-2977) cm^{-1}, as provided in Table 2. ^{1}H N.M.R. spectrum data of Mannich derivatives comprise the appearance of singlet signal of (-CH2) protons at about 4.7 ppm, multiple aromatic ring protons signals at about 6.7-8 ppm, and singlet signal of (N-H) at about 4.8 ppm, as listed in Table 3. ^{13}C-NMR data appearance about 19.2 of (CH2) aliphatic, as indicated in Table 3.

The third step,α,β–Unsaturated compounds [4-10A] were created in accordance to the crossed Aldol condensation reaction (Claisen-Schmidt reaction) [22], FT-IR spectrum of compounds [4-10A] showed the appearance of stretching bands of (C-H) olefin at (2979-2972) cm^{-1},(C=O) α,β-unsaturated ketone (1687-1656) cm^{-1}, and (C=C) olefin bands at (1569-1556) cm^{-1}, as shown in Table 2. All these bands indicate the formation of the desired chalcone derivatives. Proton nuclear magnetic resonance spectrum data of compound [4A] consisted of appearance signal of (CH=CH) protons at δ= (6.7-6.9) ppm, multi signals of aromatic rings protons at δ= (7.2-8.8), as illustrated in Table 3. ^{13}C-NMR data appearance about 121-147 (m, C aromatic), 185 (C=O), 119-120 (C=C), as indicated in Table 3.

As for compounds (11-17A), A for Oxopyrimidines derivatives was authorized by Fourier Transform Infrared Spectroscopy spectrum as well as the appearance of new bands at 1660 (C=O) belonging to the carbonyl of Oxopyrimidines, as presented in Table 2. While ^{1}H-NMR showed a signal band at 6.7 (s, 1H, Ar-NH-Oxopyrimidines ring) and also carbon-13 (C13) nuclear magnetic resonance spectra had new bands at 144-147, 26.4, and 152 follow to C=N cyclic, C-NH and C=O, respectively, demonstrated in Table 3.

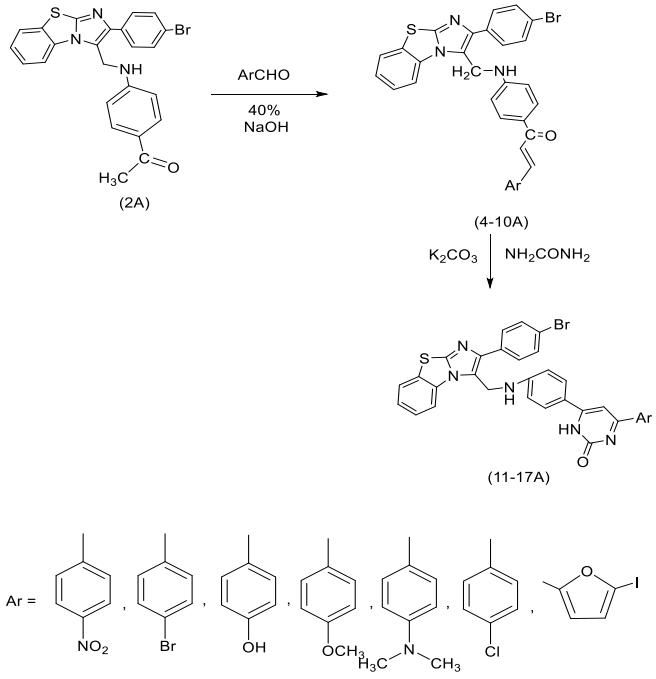

SCHEME 1 Synthesis of new Mannich bases (2-3 A) and Oxopyrimidine derivatives (11-17A)

TABLE 2 The FT-IR spectral data (Cm^{-1}) of all prepared compounds (1-17A)

Compound No.	υ (C-H) Aromatic	υ (C-H) aliphatic	υ (C=C) Aromatic	υ (C=N)	υ (C=O)	Others
1A	3055	_	1596, 1492	1639	_	υ (C-N) 1147 υ (C-Br) 642 υ (C-S-C) 746
2A	3066	2968	1595, 1492	1639	1658	υ (N-H) 3290 υ (C-N) 1338 υ (C-Br) 642 υ (C-S-C) 748
3A	3095	2977	1575, 1494	1650	1751	υ (N-H) 3396 υ (C-N) 1373 υ (C-Br) 649 υ (C-S-C) 748
4A	3070	2974	1595, 1492	1658	1683	υ (C=C) aliph. 1556 υ(NO2) asym 1523, Sym. 1357 υ(C-Br) 648 υ (C-S-C) 748
5A	3060	2972	1595, 1492	1641	1683	υ(C=C) aliph. 1558 υ(C-Br) 642 υ (C-S-C) 748
6A	3056	2979	1595, 1494	1639	1683	υ(C=C) aliph. 1560 υ (C-OH) 3431 υ (C-Br) 642 υ (C-S-C) 746
7A	3076	2979	1595, 1492	1639	1687	υ(C=C) aliph. 1562 υ (C-O) 1255 υ (C-Br) 642 υ (C-S-C) 748
8A	3070	2974	1595, 1494	1641	1658	υ(C=C) aliph. 1556 υ (C-N) 1359 υ (C-Br) 640 υ (C-S-C) 748
9A	3180	2972	1595, 1494	1639	1683	υ(C=C) aliph. 1562 υ (C-Cl) 1083 υ (C-Br) 644 υ (C-S-C) 748
10A	3058	2972	1596, 1492	1639	1656	υ(C=C) aliph. 1569 υ (C-O) 1280 υ (C-I) 680 υ (C-Br) 748 υ (C-S-C) 748
11A	3066	2974	1595, 1492	1637	1660	υ (C-N) 1180 υ (N-H) 3436 υ (C-S-C) 748 υ (C-Br) 646
12A	3068	2975	1595,1492	1639	1662	υ (C-N) 1145 υ (N-H) 3433 υ (C-S-C) 748 υ (C-Br) 642
13A	3056	2977	1593,1494	1639	1658	υ (C-N) 1178 υ (N-H) 3434 υ (C-S-C) 748 υ (C-Br) 642
14A	3072	2970	1593, 1494	1639	1670	υ (C-N) 1178 υ (N-H) 3442 υ (C-S-C) 746

15A	3001	2979	1590,1495	1639	1663	υ (C-Br) 649 υ (C-O) 1278 υ (C-N) 1176 υ (N-H) 3440 υ (C-S-C) 744
16A	3072	2970	1593, 1494	1620	1670	υ (C-Br) 64 υ (C-N) 1178 υ (N-H) 3442 υ (C-S-C) 746 υ (C-Br) 649
17A	3050	2977	1598, 1492	1639	1664	υ (C-Cl) 856 υ (C-N) 1176 υ (N-H) 3433 υ (C-S-C) 748 υ (C-Br) 640 υ (C-O) 1280 υ (C-I) 682

TABLE 3 The 1HNMR and 13CNMR spectral data (δ ppm) of compounds (2,3,10, and 17A)

Compound No.	Chemical shift
2A	^{1}HNMR: 4.8 (s,2H,CH_2NH), 4.8 (s, 1H, NH) 6.7-8 (m,12H,Ar-H), 2.6 (S,H,CH_3).
3A	^{1}HNMR 4.7 (s,2H,CH_2NH), 4.8 (s, 1H, NH) 7.4-8 (m,12H,Ar-H) ^{13}CNMR: 19.2 (CH2NH), 120-133.5 (m, 23 C aromatic),145-147 (C=N), 170.8 (C=O).
10A	^{1}HNMR: 4.7 (s, 2H, CH_2NH), 6.7-6.9 (CH=CH), 7.2-8.8 (m, 12H, Ar-H) ^{13}CNMR: 26.5 (CH2NH),119-120(CH=CH), 121-147 (m, 23 C aromatic), 152-156 (2C=N), 185 (C=O).
17A	^{1}HNMR: 4.7 (S, 2H, CH2NH), 7.3--8.0 (m, 13H, Ar-H), 6.7 (s, 1H, NH) ^{13}CNMR: 26.4 (CH2NH), 111-113 (CH=CH), 121-133.4 (23 C aromatic), 144-147 (3 C=N), 152 (C=O).

Anticorrosion

The data collected and displayed in tables and figures were used to evaluate the corrosion criterion. It was possible to obtain the corrosion potential (Ecorrosion) and current density (icorrosion) by extrapolating the cathodic and anodic Tafel in the absence and presence of the inhibitors molecules in NaCl (3.5%) solution. The anodic (2A) and cathodic (17A) Tafel slopes were also calculated from Figures 1-4 in Table 4, showing the resulting data of the potential corrosion Ecorr (mV), corrosion current density icorr (A/cm^2), cathodic and anodic Tafel slopes (mV/Dec), and protection efficiency PE%. According to a Tafel plot, the presence of inhibitors for C.S. results in a shift to a higher (noble) position, as compared with a blank solution, set up the protective laws as anodic protection. The inhibition efficiency (% I.E.) was calculated by the following equation [23,24]:

$$\%\mathbf{IE} = \frac{(\mathbf{icorr})\mathbf{o} - (\mathbf{icorr})}{(\mathbf{icorr})\mathbf{o}} * \mathbf{100} \qquad (1)$$

Where, (icorrosion) is the corrosion current density without inhibitors, and (icorrosion) is the corrosion current density with inhibitors [24,25].

Compounds (2A, 3A, 10A, and 17A) showcased a good rate of inhibition because of the adsorption of the compounds with C-steel in 3.5% NaCl. This establishes that the carbon surface atoms are bound by these atoms to prevent corrosion. In this instance, the compound atoms are prepared to bond to the carbon surface atoms, protecting the surface from corrosion.

TABLE 4 Data electrochemical of the C-steel corrosion in seawater (3.5% NaCl) for the compounds (2A,3A,10A, and 17A)

Compound No.	E corr.	I corr.	I corr./r	Resis.	Anodic β	Cathodic β	Corr. Rate,	I.E. %
Blank	-0.998	146.4	1.464E-4	523.8	0.950	0.217	0.718	-
2A(0.278)	-0.585	13.30	1.330E-5	4280	0.189	0.428	0.065	91
3A(0.4061)	-0.572	16.46	1.646E-5	3484	0.195	0.411	0.081	89
10A	-0.737	8.608	8.608E-6	4472	0.160	0.199	0.042	94
17A	-0.524	16.88	1.688E-5	2508	0.161	0.247	0.083	88

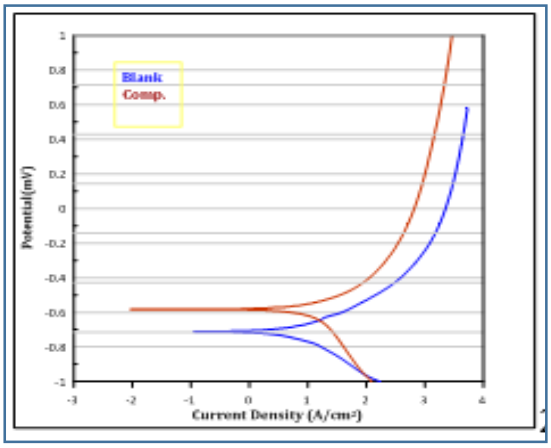

FIGURE 1 Curve of polarization of C-steel in seawater (NaCl 3.5%) of compound (2A)

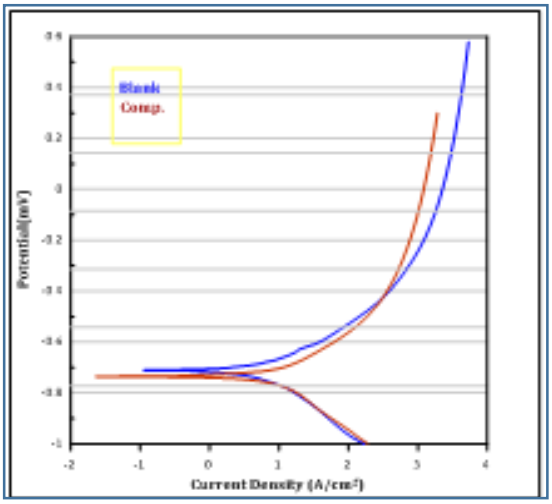

FIGURE 3 Curve of polarization of C-steel in seawater (NaCl 3.5%) of compound (10A)

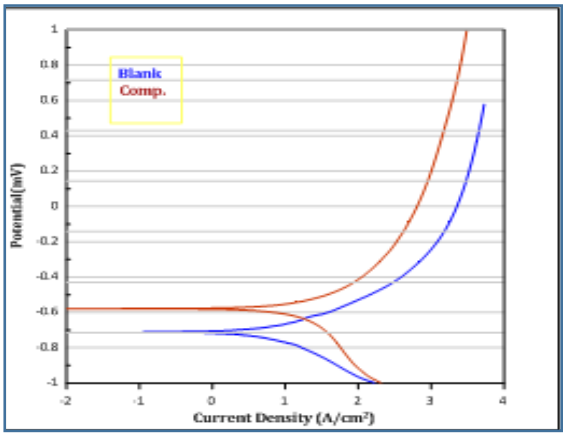

FIGURE 2 Curve of polarization of C-steel in seawater (NaCl 3.5%) of compound (3A)

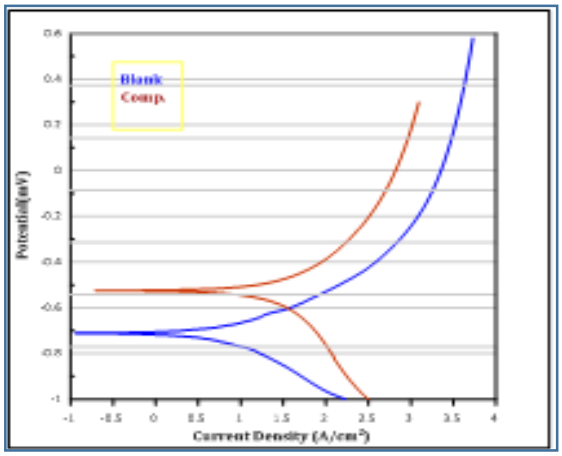

FIGURE 4 Curve of polarization of C-steel in seawater (NaCl 3.5%) of compound (17A)

Conclusion

In this work, a variety of imidazo [2,1-b] benzothiazole have been synthesized from 2-aminobenzothiazole and 4-Bromo phenacyl bromide synthesized compound (1A). As displayed in Scheme 1, while in the same scheme has been reactance 6-(4-bromophenyl) imidazo [2, 1-b] benzothiazole (1A) with different primary aromatic amines synthesized compounds (2A and 3A).

New six-membered rings of Oxopyrimidine bearing imidazo

benzothiazole fused rings were synthesized by sequence steps through Chalcones (4-10A). These new derivatives were identified by FT-IR, ^{1}H N.M.R., and ^{13}CNMR spectra. Finally, compounds (2A, 3A, 10A, and 17A) were evaluated for their anticorrosion activity on the surface of carbon steel in seawater 3.5% NaCl. These compounds exhibited good anticorrosion activity by forming an adsorbed layer on the carbon steel surface. Thus, the metal surface was protected from corrosion.

Acknowledgements

Special thanks to Senior Chemist Minera Khalid Ahmed Al-Mashhdani and Andy N. S. Shamaya for doing FT-IR spectra at the University of Baghdad.

Conflict of Interest

We have no conflicts of interest to disclose.

Orcid:

Zeena Ali Abdulameer:
https://www.orcid.org/0000-0002-1533-3559
Naeemah Jabbar Al-Lami:
https://orcid.org/0000-0002-8151-4227

References

[1] A.R. Katritzky, Y.J. Xu, H. Tu, *The Journal of Organic Chemistry*, **2003**, *68*, 4935-4937. [Crossref], [Google Scholar], [Publisher]
[2] T.A. Rehan, N. Lami, N.A. Khudhair, *Chem. Methodol.*, **2021**, *5*, 285-295. [Crossref], [Google Scholar], [Publisher]
[3] G.R. Revankar, T.R. Matthews, R.K. Robins, *J. Med. Chem.*, **1975**, *18*, 1253-1255. [Crossref], [Google Scholar], [Publisher]
[4] Y. Rival, G. Grassy, A. Taudou, R. Ecalle, *Eur. J. Med. Chem.*, **1991**, *26*, 13-18. [Crossref], [Google Scholar], [Publisher]
[5] J.B. Véron, H. Allouchia, C. Enguehard-Gueiffiera, R. Snoeck, G. Andrei, E. De Clercq, A. Gueiffier, *Bioorg. Med. Chem.*, **2008**, *16*, 9536-9545. [Crossref], [Google Scholar], [Publisher]
[6] L. Almirante, L. Polo, Alfonso [ILL], E. Provinciali, P. Rugarli, A. Gamba, A. Olivi, W. Murmann, *J. Med. Chem.*, **1966**, *9*, 29-33. [Crossref], [Google Scholar], [Publisher]
[7] C. Enguehard-Gueiffier, A. Gueiffier, *Mini Rev. Med. Chem.*, **2007**, *7*, 888-899. [Crossref], [Google Scholar], [Publisher]
[8] B. Jismy, M. Akssira, D. Knez, G. Guillaumet, S. Gobec, M. Abarbri, *New J. Chem.*, **2019**, *43*, 9961-9968. [Crossref], [Google Scholar], [Publisher]
[9] A. Kumar, M. Kumar, S. Maurya, and R. S. Khanna, *The Journal of Organic Chemistry*, **2014**, *79*, 6905-6912. [Crossref], [Google Scholar], [Publisher]
[10] E. Tret'yakova, G.S. Zakirova, E. Salimova, O. Kukovinets, V. Odinokov, L. Parfenova, *Medicinal Chemistry Research*, **2018**, *27*, 09-01. [Crossref], [Google Scholar], [Publisher]
[11] Y. Liu, Y. Dang, D. Yin, L. Yang, Q. Zou, *Res. Chem. Intermed.*, **2019**, *45*, 4907-4926. [Crossref], [Google Scholar], [Publisher]
[12] S.A. Pishawikar, H.N. More, *Arab. J. Chem.*, **2017**, *10*, S2714-S2722. [Crossref], [Google Scholar], [Publisher]
[13] A. Idhayadhulla, R.S. Kumar, A.J.A. Nasser, J. Selvin, A. Manilal, *Arab. J. Chem.*, **2014**, *7*, 994-999. [Crossref], [Google Scholar], [Publisher]
[14] A. Sharma, V. Pachauri, S.J.S. Flora, *Front. Pharmacol.*, **2018**, *9*. [Crossref], [Google Scholar], [Publisher]
[15] A.N. Vereshchagin, K.A. Karpenko, M.N. Elinson, A.S. Goloveshkin, I.E. Ushakov, M.P. Egorov, *Res. Chem. Intermed.*, **2018**, *44*, 5623-5634. [Crossref], [Google Scholar], [Publisher]
[16] P. Chao Huoa, X. Qing Guana, P. Liuc, Y. Q. Song, M.R. Sun, R.J. He, L.W. Zou, L.Juan Xue, J.Hui Shi, N. Zhang, Z.G. Liu, G. Bo Ge, *Eur. J. Med. Chem.*, **2021**, *209*, 112856. [Crossref], [Google Scholar], [Publisher]
[17] N. Aljamali, S. Hamzah Daylee, A. Jaber Kadhium, *Forefront Journal of Engineering &Technology*, **2020**, *2*, 33-44. [Crossref], [Google Scholar], [Publisher]

[18] V.V. Bhuva, *Saurashtra University*, **2009**. [Google Scholar], [Publisher]
[19] M.H. Al-Jamal, N. Al-Lami, R.M. Al-Azy, *A.I.P. Conference Proceedings*, **2020**, *2213*, 020108. [Crossref], [Google Scholar], [Publisher]
[20] J. Rostoll-Berenguer, G. Blay, J.R. Pedro, and C. Vila, *Adv. Synth. Catal.*, **2021**, *363*, 602-628. [Crossref], [Google Scholar], [Publisher]
[21] K.T. Al-Sultani, *J. Appl. Chem*., **2016**, *9*, 1-11. [Crossref], [Google Scholar], [Publisher]
[22] K.S. Gudmundsson, B.A. Johns, *Bioorganic Med. Chem. Lett.*, **2007**, *17*, 2735-2739. [Crossref], [Google Scholar], [Publisher]
[23] E. Heitz, W. Schwenk, *Br. Corros. J.*, **1976**, *11*, 74-77. [Crossref], [Google Scholar], [Publisher]
[24] T. Hoar, *J. Appl. Chem.*, **1961**, *11*, 121-130. [Crossref], [Google Scholar], [Publisher]
[25] N.A. Khudhair, A.M. Al-Sammarraie, *J. Appl. Eng. Sci.*, **2019**, *14*, 10616-10621. [Crossref], [Google Scholar], [Publisher]

How to cite this article: Zeena Ali Abdulameer*, Naeemah Jabbar Al-Lami**.** Anticorrosion activity of some new heterocyclic link with imidazo[2,1-b]benzthiazole. *Eurasian Chemical Communications*, 2023, 5(3), 271-281. **Link:** https://www.echemcom.com/article_161787.html